POLISH MARITIME RESEARCH 4 (128) 2025 Vol. 32; pp. 33-39
10.2478/pomr-2025-0048

Balanced Objective Model Predictive Control for Distance-Keeping and Tracking of Manoeuvring Vessels

Xing Wang [1,2]
Hong Yi [1,3]
Jia Xu [2]
Hailing Zhang [3]
Lifei Song [3,*]
[1] School of Ocean and Civil Engineering, Shanghai Jiao Tong University, Shanghai, China
[2] China Ship Development and Design Center, Wuhan, China
[3] Key Laboratory of Marine Intelligent Equipment and System, Shanghai Jiao Tong University, Ministry of Education, Shanghai, China
[4] Harbin Engineering University, College of shipbuilding engineering, Harbin, China

* Corresponding author: *songlifei@whut.edu.cn (L. Song)*

ABSTRACT

Maintaining a specified distance from target vessels is a common requirement in maritime management. The tracking control is inherently complex, demanding both accurate target tracking and frequent adjustments to the propeller and rudder, which can lead to increased energy consumption and accelerated mechanical wear. This study introduces a distance-keeping tracking model for manoeuvring marine vessels, along with a balanced objective model predictive control (BOMPC) algorithm. BOMPC was developed based on the Marine Manoeuvring Group (MMG) dynamics model. Beyond prioritising the tracking accuracy, the algorithm incorporates the propeller speed and rudder angle from the dynamics model as optimisation criteria within the MPC framework. This enables the simultaneous control of the tracking vessel's speed and heading, comprehensively addressing both the tracking accuracy requirements of target tracking and the considerations of energy consumption and mechanical wear. The accuracy and effectiveness of the proposed target tracking model and control algorithm are validated through both simulation and experiments. This research has potential applications in maritime management, marine search and rescue, and related domains.

Keywords: MPC, target tracking, intelligent ship, maritime management

INTRODUCTION

AShip target tracking has a broad range of applications, spanning maritime security (e.g. illegal intrusion detection, suspicious vessel defence, smuggling interdiction), maritime traffic management [1], fisheries management, maritime search and rescue, shipping logistics, and scientific research [2]. Intelligent ships are increasingly used to acquire the real-time position information of target ships and autonomously track them [3]. However, existing research in this area is primarily focused on image-based tracking, with comparatively limited attention given to maintaining a specified standoff distance when an intelligent ship is tracking a target vessel [4].

A significant challenge in ship target tracking lies in the inherent complexity and variability of the marine environment. Ships exhibit poor manoeuvrability, strong time delays, and slow control responses. The sensor accuracy and range are also limited. While target motion can be monitored, target manoeuvring capabilities are often unknown. Tracking control necessitates high manoeuvrability and adaptability, resulting in substantial energy consumption. Manual vessel operation for tracking leads to inefficient routes, frequent steering adjustments, wasted resources, and increased wear on the steering gear.

Breivik et al. [5] designed a motion control system based on the constant bearing guidance principle for tracking high-speed, linearly moving target ships. Li et al. [6] controlled speed using a fuzzy algorithm based on the relative position between an unmanned surface vehicle (USV) and the target ship, calculating the heading with reference to the optimal tracking position behind the target. Addressing the limited observation range of USVs, Zhang et al. [7] proposed a collaborative target tracking mission using an unmanned aerial vehicle (UAV) and a USV. The UAV processes aerial images to obtain the target ship's position, sending this information to the USV for rapid approach. Zhang et al. [8] presented a motion tracking method based on vision and inertial measurement units, applied to the rescue of vessels in distress, demonstrating the effectiveness of the tracking strategy. Saksvik et al. [9] achieved the real-time tracking and control of underwater gliders by exchanging data between sensors and control systems on a USV and the gliders. Teng et al. [10] combined model predictive control (MPC) with hierarchical control, demonstrating the ability to handle various constraints; however, this study aimed to replicate the target ship's motion trajectory and attitude precisely. Kim [11] designed a tracking control law with the aim of approaching the target ship as quickly as possible and also proposed an optimal motion controller for underwater target tracking, considering the USV's maximum turning rate [12]. Chen et al. [13] proposed an error-based guidance law and an adaptive Proportional-Integral-Derivative (PID) controller based on a particle swarm optimisation algorithm, but this method resulted in longer tracking distances and higher energy consumption. Agrawal et al. [14] predicted target ship paths using Monte Carlo sampling based on dynamically feasible and collision-free paths, ensuring tracking safety.

Successful target tracking requires coordinated operation between various systems, with the precise execution of commands from the decision-making system by the control system. Current ship motion control methods include sliding mode control, fuzzy control, adaptive control, MPC, robust control, Lyapunov's direct method, and backstepping design. MPC offers an excellent control performance and strong robustness, effectively mitigating process uncertainties, nonlinearities, and interactions. It also provides a convenient framework for handling various constraints on both controlled and manipulated variables [15]. However, MPC's performance is highly sensitive to the model accuracy. Li et al. [16] proposed nonlinear MPC (NMPC) and linear MPC (LMPC). NMPC addressed constrained multivariable nonlinear programming problems, while LMPC solved constrained quadratic programming problems through online iterative optimisation. Simulations demonstrated the effectiveness of MPC in ship trajectory tracking, particularly its ability to explicitly handle constraints. Yan et al. [17] designed an MPC controller for underactuated ships and employed a recurrent neural network (RNN) to address the challenges of the quadratic programming solution. Simulations demonstrated the algorithm's effectiveness and real-time performance. Wang et al. [18] developed a novel autonomous piloting and berthing system. It combines long short-term memory (LSTM) neural networks for prediction with NMPC for robust, precise vessel manoeuvring in complex environments.

Given that ships are inherently underactuated systems with limited control capabilities, significant nonlinearities, and time delays, and the uncertainties associated with target ship motion, controlling the tracking accuracy and minimising energy consumption remains challenging. This study proposes a balanced objective MPC (BOMPC) ship target range-keeping tracking algorithm to address the nonlinear and multi-constrained nature of target tracking scenarios. 'BO' signifies the balance achieved in optimising both the dynamic target tracking performance and propeller/rudder actuation, leading to reduced energy consumption and wear. By leveraging the predictive feedback capabilities of the MPC algorithm, this approach avoids excessive control adjustments, thereby increasing control stability.

TARGET TRACKING STRATEGY

The vessel acquires the real-time position information of the target ship using radar. However, radar accuracy decreases at long ranges, compromising the tracking performance. To ensure effective tracking and to avoid directly opposing the target ship's heading, a valid tracking zone is defined as a 180° fan-shaped annulus behind the target ship, as illustrated in the shaded area of Fig. 1.

In this context, T denotes the centre of the target ship, d_1 represents the maximum tracking distance, d_2 indicates the minimum tracking distance, and v_T defines the target ship's velocity vector (speed and direction). The optimal tracking distance is designated as $d_b\,(d_1 + d_2)\,/2$. A geometric approach is employed to determine the desired heading, defined as the direct line-of-sight direction between the tracking ship and the target ship. The resulting desired heading angle, Ψ_2, is calculated as follows:

$$\beta_T = \cos^{-1}\left(\frac{||BT||^2+||UT||^2-||BU||^2}{2||BT||\,||UT||}\right), \tag{1}$$

$$\Psi_2 = \Psi_T - \beta_T\,, \tag{2}$$

where β_T represents the angle between the vectors BT and UT.

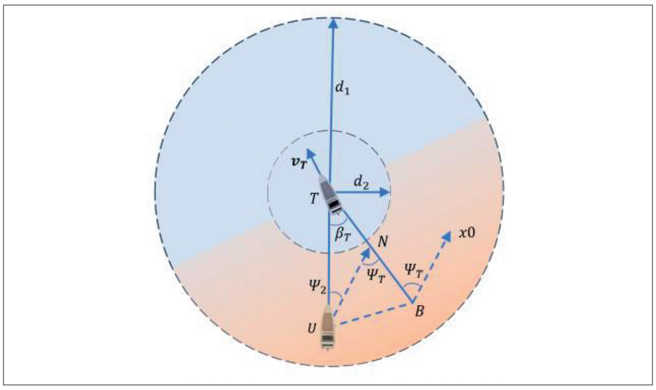

Fig. 1. Dynamic ship target tracking

This tracking strategy minimises the tracking distance, enabling the vessel to rapidly approach the target ship with minimal manoeuvring. However, sharp turns by the target ship can cause a rapid and potentially unsafe decrease in the inter-vessel distance. Therefore, a dynamic adjustment term is introduced to the optimal tracking distance:

$$d_b = \frac{d_1 - d_2}{2} + d_T \beta_T, \tag{3}$$

where d_T is the distance adjustment parameter. As β_T increases, the optimal tracking distance is increased, prompting the tracking ship to decelerate and preventing an unsafe approach to the target ship.

DESIGN OF A TARGET TRACKING HEADING AND SPEED CONTROLLER BASED ON BOMPC

First, the positions of both the tracking ship and the target ship are predicted over a defined prediction horizon. Subsequently, the desired speed and heading are calculated. Considering constraints on the rudder angle and propeller speed, a BOMPC-based speed and heading controller is designed based on the ship's Marine Manoeuvring Group (MMG) model. To address modelling uncertainties and environmental disturbances, feedback correction is applied to the prediction results. Periodic rolling optimisation is then used to obtain the optimal rudder angle and propeller speed, ensuring that the tracking ship remains within the target ship's tracking range.

TRACKING SHIP TRAJECTORY PREDICTION

Tracking ship trajectory prediction is based on the MMG model. The optimal rudder angle and propeller speed obtained from the previous time step are used as inputs. A fourth-order Runge-Kutta method is employed to solve for the tracking ship's state within the prediction horizon.

TARGET SHIP TRAJECTORY PREDICTION

Due to the unavailability of target ship Automatic Identification System (AIS) data and the difficulty in establishing a precise mathematical model for the target ship, and considering the real-time requirements of the tracking task, a constant acceleration and constant angular acceleration model is used to predict the target ship's position and velocity:

$$\begin{cases} a_{VT}(k) = \left(v_T(k) - v_T(k-1)\right)/T_c \\ a_{rT}(k) = \left(\alpha_T(k) - \alpha_T(k-1)\right)/T_c \\ \bar{v}_T(k+j|k) = v_T(k) + \Sigma_{i=1}^{j} a_{VT}(k) T_c \\ \bar{\alpha}_T(k+j|k) = \alpha_T(k) + \Sigma_{i=1}^{j} a_{rT}(k) T_c \\ \bar{x}_T(k+j|k) = x_T(k) + \Sigma_{i=1}^{j} \bar{v}_T(k+i|k) cos\left(\bar{\alpha}_T(k+i|k)\right)/T_c \\ \bar{y}_T(k+j|k) = y_T(k) + \Sigma_{i=1}^{j} \bar{v}_T(k+i|k) sin\left(\bar{\alpha}_T(k+i|k)\right)/T_c, \end{cases} \tag{4}$$

where $v_T(k)$ is the target ship's velocity at time k, $\alpha_T(k)$ is the target ship's heading, $a_{VT}(k)$ is the target ship's acceleration, $a_{rT}(k)$ is the target ship's angular acceleration, and the superscript '-' denotes a predicted value. $\bar{v}_T(k+j|k)$, $\bar{\alpha}_T(k+j|k)$, $\bar{x}_T(k+j|k)$, and $\bar{y}_T(k+j|k)$ represent the predicted values of the target ship's velocity, heading, x-position, and y-position, respectively, at time $k+j$ based on the information at time k, where $j = 1, 2,\ldots, N_p$.

SPEED CONTROLLER

The ship's MMG model is discretised:

$$\begin{cases} f_u(k) = [X_P(k) + X_R(k) + X_H(k) + (m+m_y)v(k)r(k)]/(m+m_x) \\ f_v(k) = [Y_P(k) + Y_R(k) + Y_H(k) - (m+m_x)u(k)r(k)]/(m+m_y) \\ f_r(k) = [N_P(k) + N_R(k) + N_H(k)]/(I_{ZZ}+J_{ZZ}) \\ f_x(k) = u(k) cos\Psi(k) - v(k) sin\Psi(k) \\ f_y(k) = u(k) sin\Psi(k) + v(k) cos\Psi(k) \\ f_\Psi(k) = r(k), \end{cases} \tag{5}$$

where u, v, and r are the surge velocity, sway velocity, and yaw rate, respectively; m_x and m_y are the added masses; J_{ZZ} is the added moment of inertia; X_P, Y_P, and N_P are the thrust and moments generated by the propeller; X_R, Y_R, and N_R are the forces and torques generated by the rudder; X_H, Y_H, and N_H are the hydrodynamic forces and moments acting on the bare hull; and X_G, Y_G, and N_G are the disturbance forces and moments due to wind and currents. $f_u(k)$, $f_v(k)$, $f_r(k)$, $f_x(k)$, $f_y(k)$, and $f_\Psi(k)$, are the discretised forms of $\dot{u}$, $\dot{v}$, $\dot{r}$, $\dot{x}$, $\dot{y}$, and $\dot{\Psi}$, respectively, and k indicates the current sampling time. The predicted state at the next time step is then given by

$$\begin{cases} \tilde{u}(k+1|k) = u(k) + T_C \tilde{f}_u(k|k) \\ \tilde{v}(k+1|k) = v(k) + T_C \tilde{f}_v(k|k) \\ \tilde{r}(k+1|k) = r(k) + T_C \tilde{f}_r(k|k) \\ \tilde{x}(k+1|k) = x(k) + T_C \tilde{f}_x(k|k) \\ \tilde{y}(k+1|k) = y(k) + T_C \tilde{f}_y(k|k) \\ \tilde{\Psi}(k+1|k) = \Psi(k) + T_C \tilde{f}_\Psi(k|k), \end{cases} \tag{6}$$

where the superscript '~' indicates a predicted value; and $\tilde{f}_u(k|k)$, $\tilde{f}_v(k|k)$, $\tilde{f}_r(k|k)$, $\tilde{f}_x(k|k)$, $\tilde{f}_y(k|k)$, and $\tilde{f}_\Psi(k|k)$ represent the discretised functions for predicting these states.

To reduce algorithm complexity, the speed control is simplified to controlling the surge velocity, u. Using Euler integration, the predicted ship surge velocity within the prediction horizon N_P is

$$\tilde{u}(k+j|k) = u(k) + \Sigma_{i=0}^{j-1} T_C \tilde{f}_u(k+i|k), j=1, 2,\ldots, N_P, \tag{7}$$

where $u(k)$ is the ship's surge velocity at the current time, $\tilde{u}(k+j|k)$ represents the surge velocity predicted at time $k+j$

based on the information at time k, and $\tilde{f}_u(k+i|k)$ represents the predicted $\dot{u}$ at time $k+i$ based on the information at time k. Since the surge thrust generated by the propeller is significantly greater than the surge force generated by the rudder, and to reduce the computational complexity, the rudder angle is treated as a constant in the surge velocity controller design, using its current value. The only unknown variable to be solved for is the propeller speed.

Due to modelling uncertainties and environmental disturbances, there is an error between the predicted and actual speeds. Therefore, at each new sampling time, the predicted output must be corrected using feedback. Let $e_{pu}(k-1)$ be the error between the actual and predicted surge velocity at time $k-1$. The predicted value at time $k+j$ is

$$\tilde{u}(k+j|k) = u(k)+T_C\Sigma_{i=0}^{j-1}\bar{f}_u(k+i|k) + h_u e_{pu}(k-1), \quad (8)$$

where h_u is the feedback gain.

From this, a series of desired speeds, $u_h(k+j)$, within the prediction horizon can be obtained. Combining this with Eq. (8), the speed error, $\tilde{e}_u(k+j|k)$, can be calculated:

$$\tilde{e}_u(k+j|k) = \tilde{u}(k+j|k)- u_h(k+j), j = 1, 2,\ldots, N_P. \quad (9)$$

To achieve energy savings and reduce wear from frequent propeller speed adjustments, the propeller performance must also be considered. Therefore, considering both reducing the speed error and controlling the speed input, the following optimisation function is constructed:

$$\min_{\substack{n \le n_{max} \\ |\Delta n| \le \Delta n_{max}}} f_n^*(\tilde{e}_u,n) = \Sigma_{j=1}^{N_P}\tilde{e}_u(k+j|k)\, Q_1\tilde{e}_u(k+j|k) + \Sigma_{i=0}^{N_C-1}n(k+i)\, R_1 n(k+i), \quad (10)$$

where n_{max} is the maximum propeller speed; Δn_{max} is the maximum change in the propeller speed per unit time; Q_1 and R_1 are weighting coefficients (a larger Q_1 prioritises controlling the surge velocity to reach the desired velocity, while a larger R_1 prioritises controlling the value of the propeller speed); N_C is the control horizon; and $N_C < N_P$. Setting $E_u = [\tilde{e}_u(k+1|k), \tilde{e}_u(k+2|k),\ldots,\tilde{e}_u(k+N_P|k)]^T$ and $N_R = [n(k),n(k+1),\ldots, n(k+N_C-1)]^T$ Eq. (10) can be rewritten as follows:

$$\min_{\substack{n \le n_{max} \\ |\Delta n| \le \Delta n_{max}}} f_n^*(\tilde{e}_u,n) = E_u^T Q'_1 E_u+ N_r^T R'_1 N_r, \quad (11)$$

where Q'_1 and R'_1 are diagonal matrices.

The optimisation function is a function solely of n. The optimal control quantity is solved for by optimising the function under the constraints $n \le n_{max}$ and $|\Delta n| \le \Delta n_{max}$, causing the vessel's speed to gradually approach the desired speed.

HEADING CONTROLLER

Based on Euler integration, the predicted ship heading angle within the prediction horizon N_P is given by

$$\tilde{\Psi}(k+j|k) = \Psi(k)+\Sigma_{i=1}^{j}T_C\tilde{f}_\Psi(k+i|k), j = 1, 2,\ldots, N_P, \quad (12)$$

where $\Psi(k)$ is the ship's heading angle at the current time k; $\tilde{\Psi}(k+j|k)$ represents the heading angle predicted at time $k+j$ based on the information at time k; and $\tilde{f}_\Psi(k+i|k)$ represents the predicted yaw rate. Therefore, the yaw rate must be predicted over the prediction horizon:

$$\tilde{r}(k+j|k) = r(k)+\Sigma_{i=0}^{j-1}T_C\tilde{f}_r(k+i|k), j = 1, 2,\ldots, N_P, \quad (13)$$

where $r(k)$ is the yaw rate at the current time k; $\tilde{r}(k+j|k)$ represents the yaw rate predicted at time $k+j$ based on the information at time k; and $\tilde{f}_r(k+i|k)$ is the predicted value of $\dot{r}$. The rudder angle and propeller speed in $\tilde{f}_r$ are unknown quantities to be solved for. The rudder is the primary device for controlling ship turning. Therefore, to reduce the computational complexity, the current propeller speed is substituted into $\tilde{f}_r$ when solving for the rudder angle. Substituting Eq. (13) into Eq. (12) yields the predicted heading angle:

$$\tilde{\Psi}(k+j|k) = \Psi(k)+\Sigma_{i=1}^{j}T_C\tilde{r}(k+i|k), j = 1, 2,\ldots, N_P. \quad (14)$$

Due to environmental influences and modelling inaccuracies, there is a certain discrepancy between the ship's actual heading and the predicted heading. The heading prediction error from the previous time step is used to correct the prediction for the current period:

$$\tilde{\Psi}(k+j|k) = \Psi(k)+\Sigma_{i=1}^{j}T_C\tilde{r}(k+i|k)+h_\Psi e_{p\Psi}(k-j), \quad (15)$$

where h_Ψ is the error feedback gain, and $e_{p\Psi}(k-j)$ is the heading angle prediction error at the previous time step.

Based on the predicted tracking ship position and the predicted target ship position, and using the ship's heading planning module, the desired ship heading within the prediction horizon can be obtained. The heading error can be calculated as follows:

$$\tilde{e}_\Psi(k+j|k) = \tilde{\Psi}(k+j|k) - \Psi_h(k+j), j = 1, 2,\ldots, N_P, \quad (16)$$

where $\Psi_h(k+j)$ is the desired ship heading at time $k+j$. A smaller rudder angle is more beneficial for ship safety. Therefore, considering both the rudder angle performance and heading tracking performance, the following optimisation function is constructed:

$$\min_{\substack{\delta_{min} \le \delta \le \delta_{max} \\ |\Delta\delta| \le \Delta\delta_{max}}} f_\delta^*(\tilde{e}_\Psi,\delta) = \Sigma_{j=1}^{N_P}\tilde{e}_\Psi(k+j|k)\, Q_2\tilde{e}_\Psi(k+j|k) + \Sigma_{i=0}^{N_C-1}\delta(k+i)\, R_2\delta(k+i), \quad (17)$$

where δ_{max} and δ_{min} are the maximum and minimum rudder angles, respectively; $\Delta\delta_{max}$ is the maximum rudder angle change per unit time; and Q_2 and R_2 are weighting coefficients (a larger Q_2 prioritises controlling the ship's heading to reach the desired heading, while a larger R_2 prioritises controlling the magnitude of the rudder angle). Let $E_\Psi = [\tilde{e}_\Psi(k+1|k), \tilde{e}_\Psi(k+2|k),\ldots, \tilde{e}_\Psi(k+N_P|k)]^T$ and $\delta_r = [\delta(k), \delta(k+1),\ldots, \delta(k+N_C-1)]^T$. The above equation can be written as

$$\min_{\substack{\delta_{min} \le \delta \le \delta_{max} \\ |\Delta\delta| \le \Delta\delta_{max}}} f_\delta^*(\tilde{e}_\Psi, \delta) = E_\Psi^T Q'_2 E_\Psi + \delta_r^T R'_2 \delta_r , \quad (18)$$

where Q'_2 and R'_2 are diagonal matrices.

The optimisation function is a function solely of δ. The rudder angle is solved for by optimising the function under the constraints $\delta_{min} \le \delta \le \delta_{max}$ and $[\delta(k-1)-\Delta\delta_{max}] \le \delta(k) \le [\delta(k-1)+\Delta\delta_{max}]$, causing the tracking ship to reach the desired heading.

EXPERIMENTS AND RESULTS ANALYSIS

SIMULATION

To validate the effectiveness of the proposed target tracking strategy, simulations were conducted using the 5415 standard model to simulate target tracking under the influence of wind and currents. Key simulation parameters included the following: $N_P = 10$, $N_C = 1$, $T_C = 1\ s$, $\Delta n_{max} = 0.5\ r/s$, $\delta_{min} = -35°$, $\delta_{max} = 35°$, $\Delta\delta_{max} = 9°/s$, $d_1 = 500\ m$, $d_2 = 300\ m$, current velocity $V_C = 1.5\ m/s$, current direction $\Psi_C = 180°$, wind speed $U_T = 7\ m/s$, and wind direction $\Psi_T = 0°$.

Fig. 2 illustrates the trajectories of both the tracking ship and the target ship throughout the simulation, highlighting their kinematic states at 130 s, 210 s, 325 s, 500 s, and 600 s. The target ship followed an approximately square-wave trajectory, while the tracking ship maintained a target range of 400 m. The gradient-coloured, semi-circular annulus surrounding the target ship represents the accepTable tracking range, with darker shades indicating more favourable angular positions for the tracking ship. As shown by the curves in Fig. 3, the tracking range transitioned from 500 m to the optimal 400 m range at 74 s. Fluctuations in the tracking range occurred during periods of significant course alteration by the tracking vessel. These fluctuations were addressed through substantial adjustments to the tracking ship's propeller pitch, resulting in corresponding velocity modulations to maintain the tracking range within accepTable bounds. Concurrently, as depicted in Fig. 4, the tracking vessel's rudder angle was adjusted frequently and smoothly within its operational limits, enabling smooth adjustments to the vessel's heading. These results collectively demonstrate the effectiveness and robustness of the proposed tracking strategy.

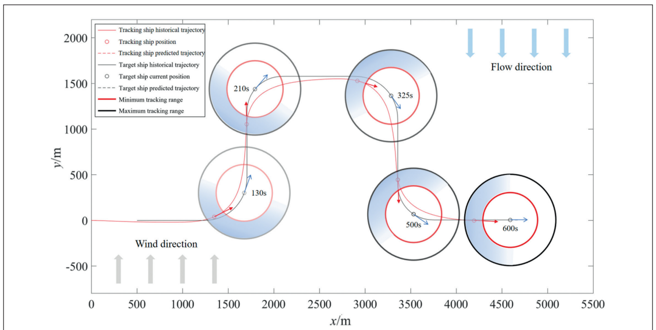

Fig. 2. Trajectory tracking performance

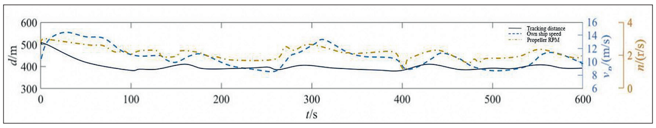

Fig. 3. Time-series representation of tracking range, tracking ship speed, and propeller rotational speed

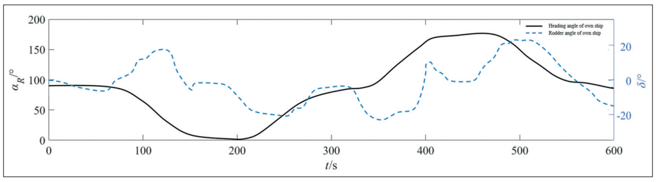

Fig. 4. Time-series representation of tracking vessel heading and rudder angle

EXPERIMENTATION

As illustrated in Fig. 5, an experimental platform was constructed based on the hull model of a 5415 standard model. The tracking vessel featured a 2 m hull length and employed dual real-time kinematic (RTK) GPS receivers, positioned at the bow and stern, for high-precision localisation. Data acquisition and command execution were managed by an STM32 embedded device. A dedicated industrial PC (IPC), running the Ubuntu operating system, executed the control algorithms and decision-making processes. Wireless communication between the IPC and a shore-based host computer was facilitated via a wireless network adapter. The model was equipped with a forward-facing visual camera with a 45-degree field of view, enabling real-time image acquisition. Communication and algorithm implementation within the Ubuntu environment were based on the Robot Operating System (ROS). The target ship, a USV, autonomously navigated a pre-defined sinusoidal trajectory. Given the reduced scale of the vessels, the optimal tracking range was established within a 3-metre to 7-metre band, centred around a target range of 5 m.

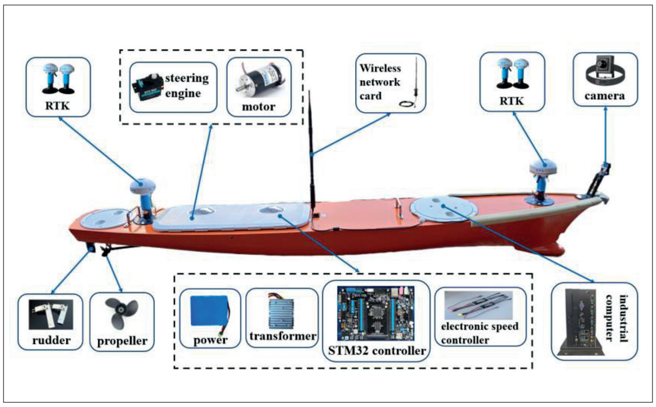

Fig. 5. The 5415 standard ship model experimental platform

Fig. 6 presents the experimental environment visualised in RViz on the shore-based host computer. Real-time video from the tracking vessel's forward-facing camera is displayed on the left side, while the right side shows the dynamically updated navigation trajectories of both the tracking and target vessels, obtained via RTK positioning. An aerial perspective, provided by a drone-mounted camera, offers a comprehensive overview of the two vessels during operation.

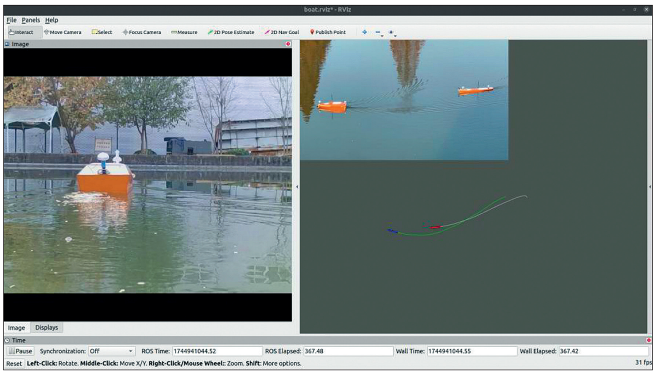

Fig. 6. Experimental scenario and vessel trajectories visualised in RViz

Fig. 7 comparatively illustrates the target ship's trajectory alongside those of the tracking ship under the control of both an adaptive PID and the proposed BOMPC algorithm. To highlight key performance differences, specific time points (24 s, 35 s, and 68 s), corresponding to the maxima of the target vessel's sinusoidal trajectory, are annotated. At these points, the positions of the target ship, the PID-controlled tracking ship, and the BOMPC tracking ship are presented. The results demonstrate that the BOMPC-controlled ship rapidly adjusts its speed while simultaneously maintaining a high steady-state accuracy, exhibiting superior dynamic response characteristics compared to its PID-controlled counterpart. Furthermore, the BOMPC-driven velocity and rudder angle adjustments are smoother, minimising the frequency of control actions and reducing the overall energy consumption. The BOMPC controller accurately tracks the line-of-sight (LOS) angle, resulting in smooth heading adjustments that avoid overshooting and oscillations, thereby enhancing the target-following precision. An analysis of roll angle variations reveals significant differences in disturbance rejection capabilities, with the MPC minimising excessive roll induced by abrupt rudder manoeuvres, which can compromise vessel stability. Throughout the tracking process, the BOMPC algorithm consistently maintained the tracking range within the defined bounds, a performance not consistently achieved by the adaptive PID algorithm. Collectively, these findings demonstrate that the enhanced MPC algorithm significantly outperforms the adaptive PID algorithm in terms of speed regulation, lateral stability, path-following accuracy, and the dynamic response of both the propeller and rudder. This superior control performance, characterised by efficiency, smoothness, and precision, makes BOMPC particularly well-suited for complex path-following scenarios.

CONCLUSION

This study introduces a BOMPC algorithm for ship target tracking. The proposed method integrates a kinematic model for maintaining a desired tracking distance with an MPC model based on the MMG model. This framework not only anticipates and satisfies the tracking control requirements but

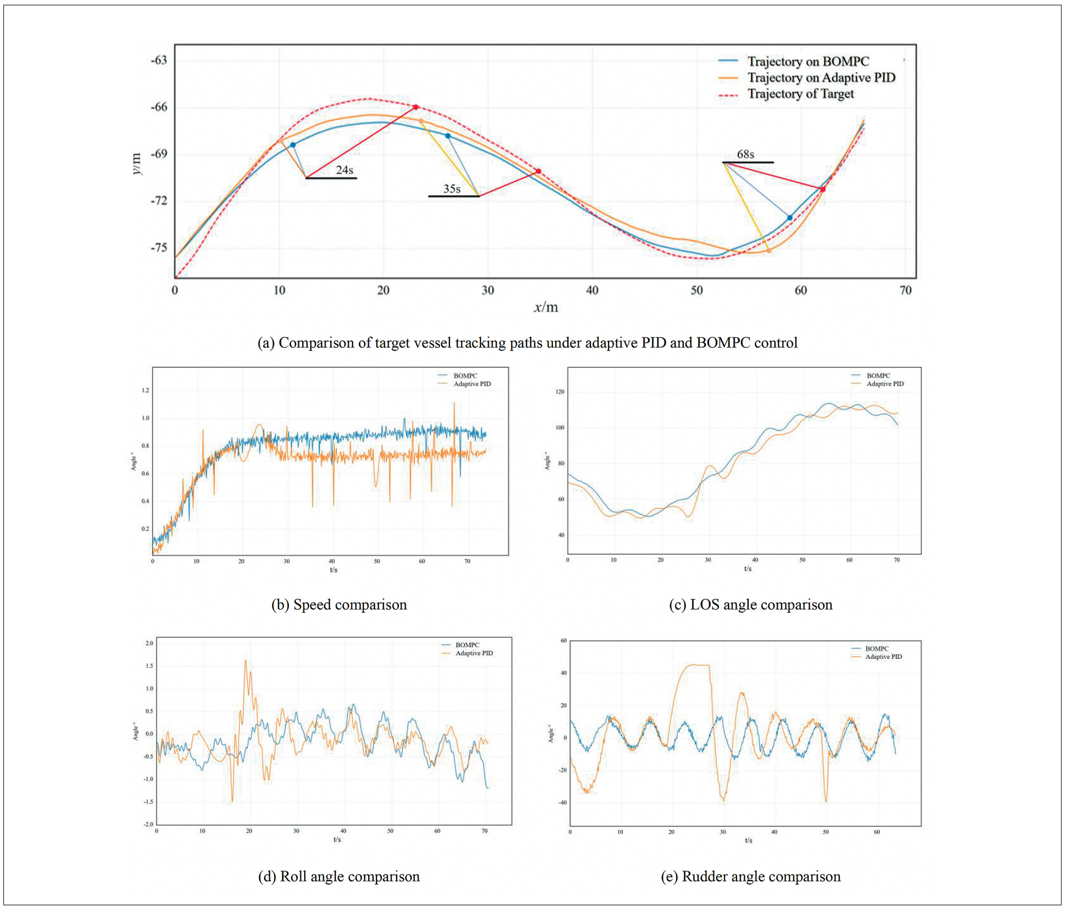

Fig. 7. Data from target vessel distance-keeping tracking experiment

also optimises propeller speed and rudder angle control during speed and heading regulation. The resulting control enables the tracking vessel to maintain a pre-defined distance behind the target vessel with excellent control continuity, minimal energy consumption, and reduced mechanical wear on both the propeller and rudder. This research has broad applications in maritime traffic management, search and rescue operations, and maritime security, specifically in scenarios requiring the effective tracking of target vessels.

ACKNOWLEDGMENT

This work is supported by the Fundamental Research Programme Grant (JCKY2023206A023).

REFERENCES

1. Han S, Sun JH, Zhou L. A potential field-based model predictive target following controller for underactuated unmanned surface vehicles. IEEE Transactions on Vehicular Technology 2024, 73(10): 14510–14524.
2. Guo R, Mao Y, Xiang ZQ. Research on LSTM-based maneuvering motion prediction for USVs. Journal of Marine Science and Engineering 2024, 12, 1661. https://doi.org/10.3390/jmse12091661
3. Zhang H, Huang Y, Qin H, Geng Z. USV search mission planning methodology for lost target rescue on sea. Electronics 2023, 12(22): 4584. https://doi.org/10.3390/electronics12224584
4. Er MJ, Ma C, Gong HB. Intelligent motion control of unmanned surface vehicles: A critical review. Ocean Engineering 2023, 280: 115113.
5. Breivik M, Hovstein VE, Fossen TI. Straight-line target tracking for unmanned surface vehicles. Modeling, Identification and Control 2008, 29(4): 131–149. https://doi.org/10.4173/mic.2008.4.2
6. Li LG, Pei ZY, Jin JC, Dai YS. Control of unmanned surface vehicle along the desired trajectory using improved line of sight and estimated sideslip angle. Polish Maritime Research 2021, 28(2): 18–26. https://doi.org/10.2478/pomr-2021-0017
7. Zhang WJ, Wang FQ, Gao QQ, Qu XR. Navigation situation assessment of autonomous surface vehicles in a cooperative hunting environment. Polish Maritime Research 2022, 29(2): 19–26. https://doi.org/10.2478/pomr-2022-0013
8. Zhang YY, Wang ZH, Zou ZJ. Black-box modeling of ship maneuvering motion based on multi-output nu-support vector regression with random excitation signal. Ocean Engineering 2022, 257, 111279.
9. Saksvik IB, Alcocer A, Hassani V. Target tracking of an underwater glider using a small unmanned surface vessel. IFAC-PapersOnLine 2022, 55(31): 478–483.
10. Teng Y, Liu Z, Zhang L, et al. On intelligent ship tracking control method based on hierarchical MPC. Proceedings of the 2021 40th Chinese Control Conference (CCC). IEEE, 2021: 2814–2819.
11. Kim J. Target following and close monitoring using an unmanned surface vehicle. IEEE Transactions on Systems, Man, and Cybernetics: Systems 2020, 50(11): 4233–4242.
12. Kim J. Optimal motion controllers for an unmanned surface vehicle to track a maneuvering underwater target based on coarse range-bearing measurements. Ocean Engineering 2020, 216: 107973. https://doi.org/10.1016/j.oceaneng.2020.107973
13. Chen Z, Guo Y, Wang Q. Research on target tracking system of unmanned surface vehicle based on hierarchical control strategy. Proceedings of the 41st Chinese Control Conference (CCC). IEEE, 2022: 3651–3655.
14. Agrawal P, Dolan JM. COLREGS-compliant target following for an unmanned surface vehicle in dynamic environments. Proceedings of the IEEE/RSJ International Conference on Intelligent Robots and Systems (IROS). IEEE, 2015: 1065–1070.
15. Han S, Yan LX, Sun JH, Ding SF, Li F, Zhou L. Automatic unberthing for underactuated unmanned surface vehicle: Model-based planning and control approaches in constricted harbors. Ocean Engineering 2024, 312: 119059.
16. Li SJ, Liu JL, Wu Q. Automatic docking for underactuated ships based on multi-objective nonlinear model predictive control. IEEE Access 2020, 8: 70044–70057.
17. Chen HZ, Yan HC, Zhang D. Reinforcement learning-based close formation control for underactuated surface vehicle with prescribed performance and time-varying state constraints. Ocean Engineering 2022, 256: 111361.
18. Wang SZ, Sun ZY, Hsieh TH. Autonomous piloting and berthing based on long short time memory neural networks and nonlinear model predictive control algorithm. Ocean Engineering 2022, 264(10):112269.